Elsevier Editorial System(tm) for Applied Thermal Engineering
Manuscript Draft

Manuscript Number:

Title: A review of natural convective heat transfer correlations in rectangular cross-section cavities and their potential applications to compound parabolic concentrating (CPC) solar collector cavities

Article Type: Review Article

Keywords: Heat transfer; Solar; Compound Parabolic Concentrator (CPC); Natural convection; Rayleigh number; Nusselt number

Corresponding Author: Dr Harjit Singh, PhD

Corresponding Author's Institution: Kingston University London

First Author: Harjit Singh, PhD

Order of Authors: Harjit Singh, PhD; Philip C Eames, PhD

Abstract: Natural convective heat transfer in cavities is a complex function of cavity shape, aspect ratio, boundary conditions at the walls and the properties of the fluid contained within the enclosure. Considerable research into natural convection in regular shaped cavities, such as those of rectangular, square cross-section, or cylindrical annuli has been undertaken. Knowledge is, however, more limited relating to natural convective heat transfer in CPC solar collector cavities. Accurate knowledge of the variation in local convective heat transfer coefficients at the different CPC cavity components would facilitate to the design of suitable convection suppression devices, for example baffles at specific locations within the cavity, substantially reducing convective heat transfer and thus improving the performance of CPC solar collectors. From analysis of the correlations developed for regularly shaped enclosures it is concluded that the employment of these correlations to describe natural convection in CPC solar collector cavities can be misleading.

1. Introduction

Natural convective heat transfer within differently shaped enclosures with varying wall boundary conditions at heated and cooled walls has been the subject of considerable research since the first reported studies by Benard [1] and Rayleigh [2]. In the literature numerous analytical and experimental studies into heat transfer in regular shaped enclosures, including rectangular or square cross-section and cylindrical annuli are detailed. The reported nature of convective flow is a complex function of the shape, orientation and aspect ratios of the enclosure, the Prandtl number of the fluid and the thermal boundary conditions prevailing at the enclosure walls. These correlations were developed for specific cross sections and are not directly applicable to natural convective flow and heat transfer in a CPC solar collector cavity formed by the absorber, aperture cover, reflector side walls and end walls. Previous studies on CPCs report measurements of air velocities, and detail the air flow distributions within cavities, temperature distributions and heat transfer phenomena are not addressed with a similar level of detail. To date only the effect of transverse tilt has been documented in the literature, the effects of longitudinal tilt are neglected. No studies have analysed the effects of convection in line-axis CPC solar collectors simultaneously inclined in both the longitudinal and transverse axes. The assumption that the correlations obtained to characterise natural convection in regular shaped (rectangular or cylindrical annuli) cavities are sufficient and appropriate for application to the cavity of a CPC solar collector [3,4,5] is challenged here.

2. Heat transfer in line-axis CPC solar collectors

Heat exchange between various elements of a CPC solar collector cavity is a complex combination of conduction, convection and radiative heat transfer. For a CPC solar collector working at a temperature of 100 ºC or higher with a high performance selectively coated absorber, natural convection within the cavity (from the hot absorber to the cold aperture cover and walls) is the dominant mode of heat transfer [6]. Fig. 1 illustrates the components of heat transfer in a line-axis concentrating CPC solar collector.

Heat transfer in non-imaging line-axis solar collectors comprises the following:

- Absorption of incident solar radiation at collector components, aperture cover, reflector walls, end walls, absorber and absorber cover if present
- Conductive heat transfer in all collector components

- Transfer of heat to the collector heat removal fluid from the absorber by conduction and convection
- Radiative and convective heat transfer to the ambient environment from the collector components
- Natural convective heat transfer between the collector cavity boundaries and the enclosed air
- Long wave radiative exchange between collector components that view each other

A major consideration solar collector designers have is to reduce the heat loss from the hot absorber to the cooler ambient environment. Conduction in the absorber, reflector walls, end walls and the aperture cover combined with solar energy input and long wave radiative heat transfer has a significant effect on the natural convective motion of air within the collector cavity. Long wave radiative heat loss from the absorber can be reduced by a large extent by employing a selective absorber surface characterised by high solar absorptance (>0.9) and low long-wave emittance (<0.1). In a solar collector with a selective coated absorber surface natural convection is the dominant component in the total heat loss [6]. Although several analytical and experimental studies have been performed, natural convective heat transfer in CPCs can still not be confidently predicted over the full parametric range of interest. In practice a CPC solar collector is installed at an angle of inclination based upon the latitude of the site of location, either in an E-W or in a N-S alignment with respect to the longer axis of the absorber. In both cases, for an absorber without an evacuated envelope, the temperature difference between the warmer absorber and colder cover and cavity walls gives rise to buoyancy forces, which establish and drive natural convective heat transfer within the air enclosed in the collector trough. Convection must be suppressed if high absorber temperatures are to be achieved and system efficiency enhanced.

3. Typical shape, geometry (aspect ratios) and orientation of enclosures employed previously to describe natural convective phenomena in cavities

A review of the literature has revealed many studies detailing experimental and numerical investigations into natural convective heat transfer in enclosures with shapes relevant to CPC geometries, such as rectangular, V-trough and cylindrical enclosures, with a range of different parametric and boundary conditions. Enclosures with walls that are perpendicular to adjoining walls are described as rectangular enclosures and include two-dimensional rectangular, two-dimensional square and three-dimensional cubical enclosures. Enclosures can be either horizontal, vertical, transversely tilted or longitudinally tilted as illustrated in Fig. 2. In the horizontal orientation (Fig. 2a) the horizontal walls of the cavity are heated differentially whilst the sidewalls and end walls can have a range of thermal and flow boundary conditions. In the vertical orientation shown in Fig. 2b, any two opposite vertical walls of the cavity are heated differentially whilst the horizontal and end walls can have a range of thermal and flow boundary conditions. In a tilted enclosure, differentially heated surfaces make an oblique angle with the horizontal plane (Fig. 2c and 2d). Fig. 3 shows the cross-sections of CPC and V-trough solar collector cavities reported in previous selected studies. Relevant aspect ratios are also detailed on figures 2 and 3.

4. Effect of enclosure shape, geometry and orientation, and thermal boundary conditions at cavity surfaces on natural convective flow in cavities

Commonly employed side wall thermal boundary conditions include adiabatic or conducting with the later resulting in a linear temperature profile (LTP) in the walls. Two mechanisms leading to three-dimensional steady flow of a fluid (Pr = 0.1-100) in the presence of no-slip side walls were presented in [14]. The first was the interaction of a rotating fluid with a stationary wall where inertial forces induced an axial velocity within the rotating fluid. The second mechanism, called the thermal end effect, resulted from temperature gradients normal to the vertical walls. It was found that while the three-dimensionality caused by the thermal effects is restricted to a small zone near the walls, the inertial effect caused the three-dimensional flow to fill the whole box. As the Prandtl number increased the inertial effects became less and less important. For moderate values of the Rayleigh number ($Ra \leq 1\times10^6$), the axial motion was found to be inertia free for a fluid with $Pr \geq 7$ [15] and $Pr \geq 10$ [14]. In a Newtonian or real fluid contained in a horizontally oriented rectangular enclosure (heated from below and cooled from above) with insulated side walls the onset of convection is characterised by longitudinal rolls with their axes perpendicular to the longer side [16,17,18,19]. The flow patterns in CPC and V-trough collector cavities are reported to consist of transverse roll-cells unlike the rectangular cross-section cavities, which exhibit longitudinal roll-cells at the initiation of the convective flow, for similar aspect ratios and thermal boundary conditions. That the boundary conditions play a significant role in deciding the dimensionality of fluid flow was shown experimentally [17] where three-dimensional natural convective roll-cells in glycerine contained in a square channel (A_x =1, A_z = 20) was observed with conducting side walls and two-dimensional roll-cells with axes perpendicular to the longer wall when side walls were insulated. For an enclosure with a square plan form, the axis of the roll-cell was found to be perpendicular to the wall with the highest thermal conductivity, indicating a clear dependence on the wall thermal boundary conditions [20]. Three-dimensional convective motion in an enclosure (A_x =0.25,0.5 and A_z = 12) with side walls having a LTP was reported by Catton [16]. Conduction within the side walls and radiative exchange between the walls of the enclosure was found to inhibit longitudinal motion by thermally stratifying the fluid and increasing the value of critical Rayleigh number [21,22]. The presence of a unicellular convective flow pattern was reported by Hernandez and Frederick [23] and bi-cellular flows by Corcione [24] in enclosures with $A_x = 2$ and adiabatic side walls indicate that past studies have reported conflicting results. Both [23, 24] were numerical studies and were not accompanied by any validating experimental results. The effect of aspect ratio is evident from the results of [23] who reported unicellular flows in square cross-section enclosures with $A_x = A_z = 1, 1.5, 2$ at $Ra = 8\times10^3$ and a multicellular flow pattern consisting of concentric roll-cells for enclosures with $A_x \geq 3$ and $A_z \geq 3$ in Rayleigh-Benard convection of air. A single cell flow pattern in enclosures with $A_x = 0.66$- 1, and a multi roll-cell structure as the aspect ratio was increased to $A_x \geq 2$ was reported by [24].

In the case of vertically oriented enclosures any temperature difference between the active vertical walls was found to give rise to convective fluid motion, a situation called dynamic type instability [25]. The strength of the rotational flow and end effect was found to be a function of the longitudinal aspect ratio (A_z) [14]. For air, flow was found to be three-dimensional in the full cavity with $A_x = 1$ and $A_z \geq 1.2$ at $6\times10^4 \leq Ra \leq 1\times10^6$. It was concluded that flow in a high Prandtl ($Pr \geq 10$) number fluid contained in a cavity with $A_x > 1$ at high Rayleigh number would be two-dimensional. It was reported that flow in a differentially heated vertical square cross-section cavity can be regarded as two-dimensional provided $A_z \geq 2$ and the horizontal surfaces and end walls are perfectly insulated for $Ra < 1\times10^7$ [26]. At $Ra = 1\times10^6$, the conductive heat transfer in the end walls was found to have a negligible effect on the observed flow structures and heat transfer rate in water contained in a cavity with $A_x = 1$ and $A_z = 2$, but a considerable effect in the case of air.

A tilted fluid layer is thought to be subjected to two types of instabilities, the static top-heavy type associated with a horizontal layer and the dynamic type, which applies to the vertical slot. At low angles of tilt (from the horizontal) the static top heavy type instability comes into play first and at angles of tilt near the vertical and beyond, the dynamic type. At some intermediate angle known as the critical angle, θ_c, cross over from one type of instability to the other takes place. For angles of inclination smaller than the critical angle, the instability is mainly buoyancy driven and leads to longitudinal rolls superimposed on the base flow. For angles of inclination between θ_c and 90º, the instability is mainly hydrodynamic and leads to transverse rolls. There is an intricate superposition of base flow and transverse or longitudinal convection roll-cells with a resultant flow that is three-dimensional in nature. The minimum aspect ratio required to render two-dimensionality to an enclosure was reported to depend upon the Prandtl number of the fluid contained in the enclosure [25]. For air in a differentially heated vertical enclosure, satisfying the inequality, $A_z > 30Pr$, was found to be sufficient to ensure two-dimensionality of flow in the enclosure. For a tilted enclosure the critical Rayleigh number was reported to be $Ra_c = 1708/\cos\theta$ and the critical tilt angle was found to be a strong function of the Prandtl number. Values of longitudinal aspect ratio that would render two-dimensionality to the natural convection phenomena in rectangular enclosures, similar to flat plate solar collector cavities, were proposed by a range of past researchers; $A_z = 12$ for a Boussinesq fluid with $\Pr \geq 10$ in cavities with $A_x = 2$ [27], $A_z > 12$ for air in cavities with $8 \leq A_x \leq 23$ [28], $A_z = 7.5$ for air in cavities with $5 \leq A_x \leq 110$ [29]. The studies due to [27,28] employed adiabatic side walls whereas [29] used LTP conditions on the side walls. Lee et al. [30] proposed this limit to be equal to the ratio of the radii of the two cylinders of 2.6-3.0 for eccentric or concentric annuli. Degaldo-Buscalioni and Crespo del Arco E. [31] concluded that thermal three-dimensional instabilities may develop if the third dimension of the cavity is typically more than twice its height. In a theoretical and experimental study natural convective flow of air contained in a large two-dimensional ($A_x = 48$) transversely tilted cavity (ϕ=0-60º) was found to comprise a base flow having a single roll-cell rising near the hot surface and falling near the cold for $Ra < Ra_c$ [4]. The results of [4, 28,29] are more relevant to flat plate solar collectors. For smaller aspect ratio enclosures ($A_x = 0.17$) convective flow was reported to consist of multi longitudinal roll-cells for enclosures tilted at $\phi \leq 70$º which shift to a single roll-cell flow at $\phi = 70$º for a rectangular cavity with insulated side walls and $A_x = 0.17$ [32]. Symons and Peck [32] experimentally found that the transition from a multiple roll-cell to a unicellular flow pattern in air contained in a rectangular cavity ($A_x = 0.17$) at $Ra = 3\times 10^5$ occurred at $\phi \leq 70$º when the cavity was tilted transversely and at $\theta = 24$º when it was tilted longitudinally. Linthorst et al. [33] reported experiments on air contained in a rectangular enclosure ($0.25 \leq A_x \leq 73$ and $A_z = 5, 10$) and concluded that for cavities with $A_x < 1$ transition to three-dimensional flow occurred if A_x decreased with a simultaneous increase in tilt angle. For cavities with $A_x \geq 1$ transition took place when A_x was increased with a simultaneous increase in tilt angle. A simultaneous Laser Doppler Anemometry study showed that a value of $A_z = 5$ was large enough to cause two dimensional flow of air at the mid-plane of a vertical cavity. Catton et al. [34] reported that for tilted cavities, increasing the aspect ratio induced a transverse fluid motion which increased convective heat transfer. Enclosures with side walls having a LTP inhibited longitudinal fluid motion for $A_x \leq 1$ and smaller values of transverse tilt angle. Enclosures with adiabatic side walls were found to inhibit these effects for large values of aspect ratio, $A_x > 1$, and transverse tilt angle. A numerical study [35] of laminar and turbulent natural convection in air contained in a two-dimensional transversely tilted square cavity predicted transition from two-dimensional to three-dimensional laminar flow to take place at close to ϕ = 20º at $Ra = 1\times 10^6$ and to turbulent flow at close to ϕ = 0º at $Ra = 1\times 10^{10}$. Conflicting reports about convective roll-cell patterns in CPC solar collector cavities were published by [7,8]. For example, under the same boundary conditions and Rayleigh number range, $1\times10^3 \leq \mathrm{Ra} \leq 2.5\times10^6$, in [8] they predicted a single transverse roll-cell pattern in a horizontally oriented 1/3 height CPC solar collector (C_R =2, A_x =1.91) cavity and a double roll-cell pattern in [7]. A single transverse roll-cell in the cavity of a transversely tilted (ϕ=30-90º) V-trough solar collector with C_R = 2,3,4,5 (A_x = 0.44-2.1) and insulated side walls over the range $Ra \leq 10^7$ was observed [9]. The flow was found to be laminar up to $Ra = 10^7$. In a numerical study [11] two-dimensional natural convection in the cavity of a transversely tilted (ϕ = 0, 15, 30, 60, 90º) CPC collector with CR = 2, the convective flow pattern was found to be a function of the tilt angle, the Grashof number (Gr) and the height of the collector cavity for $Gr = 5\times10^4$. Flow patterns were found to be bicellular for collectors with 1/3, 2/3 and full height just after the initialization of convection. The flow pattern in a 1/3 height CPC cavity was found to be bicellular for tilt angles up to 15º, at all Grashof numbers, beyond which it became unicellular. For taller collectors the flow changed from transverse bicellular to a unicellular pattern over the range $5\times10^3 \leq Gr \leq 5\times10^4$ at a transverse tilt angle between ϕ = 0º and ϕ = 15º. The effect of thermal boundary conditions on the side walls on natural convective flow of air in a CPC cavity was reported by Eames and Norton [12,13]. They reported a bicellular flow, Fig. 4, in the cavity of a 60º acceptance half-angle CPC collector (C_R = 1.15) tilted at $\phi \leq 30$º for conducting side walls with realistic back loss and a single roll cell flow for conducting side walls and adiabatic back surface (no back loss). It was reported that the tilt angle corresponding to the transition from bicellular to unicellular flow was a function of the boundary conditions and the acceptance half-angle of the CPC. The change over from bi-cellular to uni-cellular flow for the CPC with adiabatic side walls occurred at angles smaller than those for the CPC with a realistic back loss indicating the effect of the thermal boundary conditions on the natural convective flow. In CPC solar collectors with smaller acceptance half-angles of 45º and 30º (C_R = 1.41 and 2) the change from bi-cellular to a unicellular flow pattern took place at a smaller tilt angle. Truncation of the reflector walls, which results in an increase in A_x , was found to increase the angle corresponding to the transition from bi-cellular to unicellular flow for a CPC solar collector with 30º acceptance half-angle. It was concluded that the aspect ratio and not only the height of solar collector is important in determining the nature of fluid flow patterns.

The convective flow patterns of a unicellular roll-cell and a double roll-cell have been reported in CPC and V-trough solar collectors. The tilt angle corresponding to the transition from bicellular flow to unicellular flow has been found to depend on the boundary conditions and the acceptance half-angle of the CPC solar collector. The transverse aspect ratio and height of the CPC solar collectors were found to have significant effects in determining the nature of the convective f low patterns. To date, effects of longitudinal aspect ratio on the convective flow pattern within CPC and V-trough solar collectors have not been examined. The critical tilt angle, transverse or longitudinal, has been reported to be a function of temperature difference between the differentially heated sides of the enclosures and the Prandtl number of the fluid. In the case of CPC solar collector cavities filled with air, with a Prandtl number of 0.7, three-dimensional convective flow occurs due to the thermal effects and the predominant inertial effect and is likely to fill the whole enclosure and not be confined in close proximity to the physical boundaries.

5. Effect of enclosure shape, geometry and orientation, and the thermal boundary conditions prevailing at the cavity wall surfaces on natural convective heat transfer in cavities

For a horizontal cubical cavity with adiabatic lateral walls different flow structures result in different *Nu* values [36,37]. Natural convective air flow with a single transverse roll-cell yielded 65% higher heat transfer coefficients at both top and bottom plates than that for a toroidal roll-cell [36]. For tilted rectangular and V-trough enclosures, perfectly conducting side walls were found to result in smaller average Nusselt numbers than those obtained when the side walls were perfectly adiabatic for the same Rayleigh number [34,38,39]. However, the average Nusselt number at the hot wall was lower for a rectangular cavity with adiabatic side walls than that obtained when the side walls were isothermal [24]. Hot and cold walls have commonly been assumed to be isothermal [24,34,38,39]. The effect of temperature profile on the hotter surface is evident from the results of Chao et al. [40] who reported that a saw-tooth temperature profile (similar to that on the absorber of flat plate solar collectors) in the bottom surface of a rectangular cavity resulted in a higher mean Nusselt number than for a uniform temperature profile over a tilt range of $\phi \leq 90º$. The effect of radiative exchange within cavity elements has largely been neglected when reporting the results of studies into natural convective heat transfer in cavities. Kim and Viskanta [21] studied the effect of in-cavity radiative exchange on the temperature profile in air inside a horizontal square cross-section cavity and reported that the presence of radiation exchange caused different temperature profiles at the cavity surfaces than those that existed in its absence. They found that radiative exchange reduced the temperature difference between hot and cold wall resulting in smaller buoyancy forces. An increase in wall emissivity was found to decrease the average Nusselt number. Similar results were reported by [38] that side walls with lower emissivity (ε_w =0.003) resulted in a higher average Nusselt number than for those with higher emissivity (ε_w = 0.84) walls in a vertical cavity for $Ra \leq 1\times10^7$. Corcione [24] reported that at $Ra = 1\times10^5$, the average Nusselt number at the hot wall with side walls either isothermal or mixed boundary conditions (isothermal and adiabatic) approached asymptotically to that of the adiabatic side wall thermal boundary conditions as the transverse aspect ratio increased from 0.66 to 8 indicating the diminishing effect of the side wall boundary conditions as the aspect ratio increased. The local Nusselt number at the hot or cold wall was found to depend on the side wall thermal boundary conditions. It was concluded that above a certain value of Rayleigh number for a given aspect ratio, A_x, the heat transfer rate from any heated or cooled side wall is independent of the boundary condition assumed at the opposite wall. For a cavity with $A_x \geq 2$, the value was reported to be $Ra = 1\times10^5$. Hollands and Konicek [25] reported that the dimensionality of natural convective flow in a vertical enclosure is dependent on the Prandtl number of the cavity fluid. Hsieh and Wang [41] found that a longitudinal aspect ratio of $A_z = 5$ was sufficient to reduce the three-dimensional effects in the temperature distribution for vertically oriented rectangular cavities with transverse aspect ratios of A_x = 1,3 and 5. The Nusselt numbers evaluated for three-dimensional natural convective situations were found to be higher than those for two-dimensional cases. Similar results were also reported by [42,43]. The Nusselt number was reported to vary significantly with transverse and longitudinal tilt angles in enclosures that were not cubical [44]. Disagreeing significantly with these results are the results due to [9,32] with the former reporting negligible effect of transverse tilting between $30^\circ \leq \phi \leq 90^\circ$ in V-trough cavities with concentration ratios (CR) of 2 and 3 and later of longitudinal tilt over the range $0 \leq \theta \leq 15^\circ$ and $25 \leq \theta \leq 60^\circ$ on the local and mean values of Nu. Figures 5 – 10 show the variation of Nu with Rayleigh number and transverse tilt angle using correlations presented in the literature. The range covered in these figures, $1\times10^5 \leq Ra \leq 1\times10^7$ and $0^\circ \leq \phi \leq 90^\circ$, is relevant to CPC solar collectors with $1.15 \leq CR \leq 10$ [3,13,45,52]. Variation of Nu with Ra for horizontally held eccentric cylindrical annuli due to [47] exhibited no similarity with that for horizontally oriented CPC enclosures. Results published by past researchers for transversely tilted CPC solar collector cavities were compared over the range 0º (horizontal) to 90º (vertical). Figures 5-7 show the curves for 0º (horizontal), 10º and 45º transverse tilt angles. It is evident from these figures that the curves showing the variation of the Nusselt number significantly diverge from each other and the predicted values of the Nusselt number for natural convection in CPC solar collector cavities do not agree even though these correlations are drawn for a similar parametric range. It can be concluded, from the literature review, that similar or even higher discrepancies exist at all tilt positions between horizontal and vertical. The existence of similar discrepancies in the case of rectangular and eccentric annuli enclosures can be confirmed from these figures. As shown in Figure 5, the curves for horizontally oriented solar collector cavities due to [3,10,13,45] despite following a similar general trend, fail to yield values of the Nusselt number within acceptable variance of each other due to a variety of reasons such as limitations of the numerical models used, unrealistic experimental boundary conditions and differing geometries detailed in Tables 1 and 2. Natural convective heat transfer was assumed to be essentially in CPC solar collector cavities formed by isothermal absorber (heated electrically or otherwise), isothermal aperture cover and ideally reflecting side walls adiabatic at the back typical of the boundary conditions assumed in many past studies [3,5,7,8,10,45,46,49]. Rabl [3] and Abdel- Khalik et al. [7,8] assumed flat plate absorbers while the rest employed tubular absorbers in their respective studies. Chew et al. [45] reported that the experimentally measured temperatures of side walls with aluminium reflector foil ($\varepsilon_w = 0.08$) on the front face was smaller than that calculated theoretically assuming the side walls to be adiabatic. This clearly indicates that the discrepancies are caused by neglecting both the conductive and radiative exchanges within the cavity and between boundaries. Chew et al. [11] neglected the effect of radiative heat exchange between the surfaces forming the CPC cavity, others [5,12,13,21,38,45] have highlighted the effect of radiative heat exchange between the cavity surfaces on system thermal characteristics. Rabl [3] employed simplistic correlations for flat-plate film coefficients to predict natural convective heat transfer coefficients prevailing within a theoretical two-dimensional CPC solar collector cavity. In the experiments of [10] unrealistic uninsulated CPC solar collectors whose reflector walls and aperture covers were fabricated from a single polished duralumin sheet were used. Meyer et al. [9] reported that in the cavity of a V-trough solar collector with fixed concentration ratio, reduction in the Rayleigh number or increase in the concentration ratio decreased the natural convective heat transfer coefficient. The correlation due to [13] is the only correlation to date which directly correlates the Nusselt number with angle of transverse inclination, ϕ, and the geometrical dimensions of a CPC solar collector. However, this correlation is limited to uni-cellular flow situations and applies to a limited tilt angle range. The relationships for trapezoidal and V-trough cavities shown in Figures 5 and 6 clearly have no commonality with those for the CPC solar collector cavities for a similar Rayleigh number range, aspect ratio and transverse tilt angles. Even the curves for CPC solar collector cavities shown in these figures do not agree with each other within acceptable limits. Correlations developed for convective heat transfer in CPC solar collector cavities can not be used to predict the Nusselt number variation in V-trough cavities and vice-versa.

6. Effect of the Fluid Prandtl Number, *Pr*

Arnold et al. [56] concluded that fluids with $Pr \geq 4.5$ behave similarly to a fluid with infinite Prandtl number when $Ra \leq 10^7$from the perspective of heat transfer. Catton et al. [34] concluded that the infinite Prandtl number analysis is invalid for fluids with $Pr = 0.7$. Kim and Viskanta [51] found that as the Prandtl number was increased from 0.01 to 0.71 the average Nusselt number at the hot vertical wall increased by nearly 70%. The increase for Prandtl number values from 0.71 to 10 was nearly 10%. Ho et al. [50] reported a significant effect due to the Prandtl number as it changed from 0.7 to 7 on flow and local heat flux at the outer cylinder surface for an eccentric annulus arrangement with increasing Rayleigh number. Only a slight effect due to the Prandtl number was observed on the average Nusselt number for the annuli with increasing Rayleigh number. A decrease of 17% in local heat transfer coefficient was observed when the Prandtl number was changed from 0.7 to 7 at a Rayleigh number of $Ra = 1\times10^6$. Pallares et al. [37] reported that for $Ra \leq 6\times10^4$, average heat transfer rates increased as the Prandtl number increased from 0.7 to 10 but, that there was no significant change afterwards. An increase in the Prandtl number from air ($Pr = 0.71$) to higher values was found to shift the flow transitions to higher critical Rayleigh numbers. A CPC solar collector always contains air ($Pr \cong 0.71$) in its cavity. It is evident that the convective heat transfer characteristics exhibited by fluids, described by their distinctive Prandtl numbers, can not represent the case for air.

7. Effect of the Assumptions Employed for the Numerical Studies

Convective flow in a closed enclosure with comparable horizontal and vertical dimensions is always three-dimensional as a result of the no-slip conditions (zero fluid velocity relative to the solid boundary) at the vertical walls and can not be described satisfactorily by a two-dimensional model [15]. Leong et al. [43] argued that carrying out two-dimensional analysis of the natural convective flow in a square cross-section cavity will not be of much value since the two-dimensional flow is readily unstable to any three-dimensional perturbations. It has been concluded that variable property simulations can only match experimental values. The Nusselt number evaluated for more realistic three-dimensional natural convection situations was found to be higher than those predicted for simplified two-dimensional cases. The agreement between the two-dimensional numerical analysis and experimental investigation into natural convection reported by Iyican et al. [46] got progressively worse as the tilt angle approached horizontal due to the shift from predominantly two-dimensional flow to fully three-dimensional flow that would have appeared at low tilt angles. Rasoul and Prinos [59] observed a very slow convergence of their numerical model employed to predict natural convective flow of gallium (Pr = 0.2) and air (Pr = 0.71) at $Ra = 1 \times 10^6$ in a cavity for a transverse tilt of $\phi < 40^{\circ}$. They concluded that this was due to the occurrence of three-dimensional flow for this tilt range. Eames and Norton [12] reported that CPC solar collectors with aspect ratios lower than $A_x = 1.2$ and $A_z = 11.5$ could have three-dimensional convective flow. A temperature difference of 10 ºC in the heat removal water along the length of the collector was found to disrupt the convective flow in the cavity air from a two-dimensional to a three-dimensional flow. These factors when combined clearly indicate the limitations of two-dimensional models in resolving the complicated three-dimensional natural convection phenomena typical of that that occurs in CPC solar collector cavities.

8. Conclusions

(i) For similar aspect ratios and thermal boundary conditions the convective flow patterns in CPC and V-trough collector cavities are reported to consist of transverse roll-cells unlike those in rectangular cross-section cavities, which exhibit longitudinal roll-cells at the initiation of convective flow.
(ii) To date, effect of longitudinal aspect ratio on the convective flow pattern within CPC and V-trough solar collectors has not been examined.
(iii) In the case of a CPC solar collector cavity filled with air with a Prandtl number of 0.7, three-dimensional convective flow occurs due to the thermal effects and the predominant inertial effect and is likely to fill the whole enclosure and will not be confined in proximity to the physical boundaries

(iv) Convective heat transfer in enclosures is complex in nature and the correlations proposed by different researchers, even for similar operating conditions and system parameters, fail to agree on a single unifying relationship that adequately represents the variation of the Nusselt number with the longitudinal and transverse tilt angles.

(v) The complex superposition of transverse and longitudinal fluid motion has a significant effect on the magnitude of heat transfer in natural convection situations. Maxima and minima of the Nusselt number have been reported to occur at different orientations and angles of inclination by researchers when considering similar and differing operating and system parameters. Hence, the results for any particular natural convective situation can not be applied to another without significant risk of error. The shape and aspect ratios of the enclosures both have a significant effect on the angles at which the maxima and minima of the Nusselt number occur.

(vi) The Nusselt number is the most important parameter used to determine the characteristics of the natural convective heat transfer process. It has been found to be a complex function of the shape, aspect ratio, tilt angles, Rayleigh number and boundary conditions prevailing at the walls of the enclosure. The type of convective flow pattern also has an important effect on the local and average values of the Nusselt number. The Nusselt number for a two-dimensional natural convective flow has been found to be different from that for a three-dimensional flow. Considering the case of CPC solar collectors the Nusselt numbers predicted by two-dimensional models may not accurately represent Nusselt number values for convective heat transfer in reality.

(vii) The concentration ratio and truncation of reflector walls has an important effect on the convective heat transfer and the critical Rayleigh number, which signifies the onset of natural convective flow, in the case of CPC solar collectors.

(viii) Experimentally measured data detailing the temperature distribution in the three-dimensional air spaces of CPC solar collectors under realistic thermal and geometrical conditions is not available in the literature. No experimentally measured or theoretically estimated data are available in the literature to compare the relative effect of longitudinal tilt versus transverse tilt on the natural convection that occurs in CPC solar collector cavities.

(ix) The adiabatic boundary conditions assumed at the side walls of an enclosure in many previous studies are not achievable in reality. Assumed adiabatic boundary conditions lead to faulty predictions of the average Nusselt number due to their omission of conduction effects in the side walls of differentially heated enclosures. The adoption of simplifying assumptions for example neglecting the variation of temperature in the direction of the longitudinal axis of CPC solar collectors, neglecting radiative exchange between elements of the enclosure have yielded more realistic results in the past. Employing correlations derived for hot vertical and horizontal plates submerged in a fluid or assuming that convection will be similar to that within cylindrical annuli for predicting heat transfer in CPC collector cavities will yield unrealistic results.

References

[1] H. Benard, Les touribillons cellulaires dans une nappe liquid, Revue General des Sciences Pures et Appliquees 11 (1900) 1261-1271.

[2] J.W.S. Rayleigh Lord, On convection currents in a horizontal layer of fluid when the higher temperature is on the under side. Phil. Mag. 32 (1916) 529–546.

[3] A. Rabl, Optical and thermal properties of compound parabolic concentrators, Solar Energy 187 (1976) 497-511.

[4] K.G.T. Hollands, T.E. Unny, G.D. Raithby, L. Konicek, Free convective heat transfer across inclined air layers, ASME J. Heat Transfer 98 (1976) 189-193.

[5] D.E. Prapas, B. Norton, S.D. Probert, Thermal design of compound parabolic concentrating solar-energy collectors, J. Solar Energy Engineering 109 (1987) 161-168.

[6] B. Norton, Solar Energy Thermal Technology, London: Springer-Verlag London Limited, 1991.

[7] S.I. Abdel-Khalik, H.W. Li, Natural convection in inclined two-dimensional compound parabolic concentrators, in: Proc. ASME Winter Annual Meeting, San Francisco, 1978, pp. 23-28.

[8] S.I. Abdel-Khalik, H.W. Li, K.R. Randall, Natural convection in compound parabolic concentrators-A final element solution, ASME J. Heat Transfer 100 (1978) 199-204.

[9] B.A. Meyer, J.W. Mitchell, M.M. El-Wakil, Convective heat transfer in vee-trough linear concentrators, Solar Energy 28(1) (1982) 33-40.

[10] E. Prapas, B. Norton, P.E. Melidis, S.D. Probert, Convective heat transfer within air spaces of compound parabolic concentrating solar-energy collectors, Applied Energy 28 (1987) 123-135.

[11] T.C. Chew, A.O. Tay, N.E. Wijeysundera, A numerical study of the natural convection in CPC solar collector cavities with tubular absorbers, J. Solar Energy Engineering 111 (1989) 16-23.

[12] P.C. Eames, B. Norton, Validated, unified model for optics and heat transfer in line-axis concentrating solar energy collectors, Solar Energy 50(4) (1993) 339-355.

[13] P.C. Eames, B. Norton, Detailed parametric analyses of heat transfer in CPC solar energy collectors, Solar Energy 50 (4) (1993) 321-328.

[14] G.D. Mallinson, G.de Vahl Davis, Three-dimensional convection in a box: a numerical study, J. Fluid Mech. 83 (1) (1977) 1-31.

[15] R. Kessler, Non linear transition in three-dimensional convection, J. Fluid Mech. 174 (1987) 357-379.

[16] I. Catton, The effect of insulating vertical walls on the onset of motion in a fluid heated from below, Int. J. Heat Mass Transfer 15 (1972) 665-672.

[17] H. Ozoe, S.W. Churchill, Hydrodynamic stability and natural convection in Newtonian and non-Newtonian fluids heated from below, in: C. E. P. Symposium Series No. 131 Heat Transfer: Fundamentals and Industrial Applications 69 (1973) 126-133.

[18] H. Ozoe, H. Sayama, S.W. Churchill, Natural circulation in an inclined rectangular channel at various aspect ratios and angles-experimental results, Int. J. Heat Mass Transfer 18 (1975) 1425-1431.

[19] H.Q. Yang, K.T. Yang, J.R. Lloyd, Laminar natural-convection flow transitions in tilted three-dimensional longitudinal rectangular enclosures, Int. J. Heat Mass Transfer 30(8) (1987) 1637-1644.

[20] I. Catton, Effect of wall conduction on the stability of a fluid in a rectangular region heated from below, ASME J. Heat Transfer 94 (1972) 446-452.

[21] D.M. Kim, R. Viskanta, Effect of wall conduction and radiation on natural convection in a rectangular cavity, Num. Heat Transfer 7 (1984) 449-470.

[22] V.D. Murty, A numerical investigation of Benard convection using finite elements, Computers and Fluids 14(4) (1986) 379-391.

[23] R. Hernandez, R.L. Frederick, Spatial and thermal features of three-dimensional Rayleigh-Benard convection, Int. J. Heat Mass Transfer 37(3) (1994) 411-424.
[24] M. Corcione, Effects of the thermal boundary conditions at the side walls upon natural convection in rectangular enclosures heated from below and cooled from above, Int. J. Thermal Sciences 42 (2003) 199-208.
[25] K.G.T. Hollands, L. Konicek, Experimental study of the stability of differentially heated inclined air layers, Int. J. Heat Mass Transfer 16 (1973) 1467-1476.
[26] Y. Le Peutrec, G. Lauriat, Effects of the heat transfer at the side walls on natural convection in cavities, ASME J. Heat Transfer 112 (1990) 370-378.
[27] H. Ozoe, K. Yamamoto, H. Sayama, S.W. Churchill, Natural convection in a long inclined rectangular box heated from below- part II. Three dimensional numerical results, Int. J. Heat Mass Transfer 20 (1977) 131-139.
[28] K.R. Randall, J.W. Mitchell, M.M. El-Wakil, Natural convection heat transfer characteristics of flat plate enclosures, ASME J. Heat Transfer 101 (1979) 120-125.
[29] S.M. Elsherbiny, G.D. Raithby, K.G.T. Hollands, Heat transfer by natural convection across vertical and inclined air layers, ASME J. Heat Transfer 104 (1982) 96-102.
[30] T.S. Lee, N.E. Wijeysundera, K.S. Yeo, Free convective fluid motion and heat transfer in horizontal concentric and eccentric cylindrical collector systems, in: D.Y. Lowani (Ed.), Solar Engineering, Am. Soc. Mech. Eng., New York, 1984, 198, pp.194-204.
[31] R. Degaldo-Buscalioni, E. Crespo del Arco, Flow and heat transfer regimes in inclined differentially heated cavities, Int. J. Heat Mass Transfer 44 (2001) 1947-1962.
[32] J.G. Symons, M.K. Peck, Natural convection heat transfer through inclined longitudinal slots, ASME J. Heat Transfer 106 (1984) 824-829.
[33] S.J.M. Linthorst, W.M.M. Schinkel, C.J. Hoogendoorn, Flow structure with natural convection in inclined air-filled enclosures, ASME J. Heat Transfer 103 (1981) 535-539.
[34] I. Catton, P.S. Ayyaswamy, R.M. Clever, Natural convection flow in a finite, rectangular slot arbitrarily oriented with respect to the gravity vector, Int. J. Heat Mass Transfer 17 (1974) 173-184.
[35] R.A. Kuyper, ThH. Van Der Meer, C.J. Hoogendoorn, R.A.W.M. Henkes, Numerical study of laminar and turbulent natural convection in an inclined square cavity, Int. J. Heat Mass Transfer 36(11) (1993) 2899-2911.
[36] J. Pallares, I. Cuesta, F.X. Grau, F. Giralt, Natural convection in a cavity heated from below at low Rayleigh numbers, Int. J. Heat Mass Transfer 39(15) (1996) 3233-3247.
[37] J. Pallares, I. Cuesta, F.X. Grau, F. Giralt, Flow transitions in laminar Rayleigh–Bénard convection in a cubical cavity at moderate Rayleigh numbers, Int. J. Heat Mass Transfer 42(4) (1999) 753-769.
[38] S.M. Elsherbiny, K.G.T. Hollands, G.D. Raithby, Effect of thermal boundary conditions on natural convection in vertical and inclined air layers, ASME J. Heat Transfer 104 (1982) 515-520.
[39] B.A. Meyer, J.W. Mitchell, M.M. El-Wakil, The effect of thermal wall properties on natural convection in inclined rectangular cells, ASME J. Heat Transfer 104 (1982) 111-117.
[40] Chao P, Ozoe H, Churchill SW. The effect of a non-uniform surface temperature on laminar natural convection in a rectangular enclosure. Chem. Eng. Commun. 1981;9:245-54.
[41] S.S. Hsieh, C.Y. Wang, Experimental study of three-dimensional natural convection in enclosures with different working fluids, Int. J. Heat Mass Transfer 37(17) (1994) 2687-2698.
[42] S.S. Hsieh, S.S. Yang, Transient three-dimensional natural convection in a rectangular enclosure, Int. J. Heat Mass Transfer 39(1) (1996) 13-26.
[43] W.H. Leong, K.G.T. Hollands, A.P. Brunger, On a physically-realizable benchmark problem in internal natural convection, Int. J. Heat Mass Transfer 41 (1998) 3817-3828.
[44] H. Ozoe, T. Okamoto, S.W. Churchill, H. Sayama, Natural convection in doubly inclined rectangular boxes, in: Proc. 6th Int. Heat Transfer Conference vol. 2, Paper Number NC-19, 1978, pp. 293-98.
[45] T.C. Chew, N.E. Wijeysundera, A.O. Tay, An experimental study of free convection in compound parabolic concentrator (CPC) cavities, J. Solar Energy Engineering 110 (1988) 293-297.
[46] L. Iyican, L.C. Witte, Y. Bayazitoglu, An experimental study of natural convection in trapezoidal enclosures, ASME J. Heat Transfer 102 (1980) 648-653.
[47] T.H. Kuehn, R.J.Goldstein, An experimental study of natural convection heat transfer in concentric and eccentric horizontal cylindrical annuli, ASME J. Heat Transfer 100 (1978) 635-640.
[48] D.R. Smart, K.G.T. Hollands, G.D. Raithby, Free convection heat transfer across rectangular-celled diathermanous honeycombs, ASME J. Heat Transfer 102 (1980) 75-80.
[49] Tatara RA, Thodos T. Experimental natural convective studies within a compound parabolic concentrator enclosure, in: Proc. ASME Winter Annual Meeting, Miami, Florida, 1985, pp. 17-22.

[50] C.J. Ho, Y.H. Lin, T.C. Chen. A numerical study of natural convection in concentric and eccentric horizontal cylindrical annuli with mixed boundary conditions, Int. J. Heat and Fluid Flow 10(1) (1989) 40-47.
[51] D.M. Kim, R. Viskanta, Study of the effects of wall conductance on natural convection in differently oriented square cavities, J. Fluid Mech. 144 (1984) 153-176.
[52] H. Singh, An experimental study of natural convective heat flow phenomena in concentrating compound parabolic solar collector cavities, PhD Thesis, University of Ulster, UK, 2009.
[53] A. Fasulo, L. Odicino, D. Perello, Development of a CPC with low thermal losses. Solar Wind Tech. 4 (2) (1987) 157-162.
[54] Y.P. Yadav, A.K. Yadav, N. Anwar, P.C. Eames, B. Norton, The fabrication and testing of a line-axis compound parabolic concentrating solar energy collector, in: Proc. WREC, 1996, pp. 572-575.
[55] P.C. Eames, M. Smyth, B. Norton, The experimental validation of a comprehensive unified model for optics and heat transfer in line-axis solar energy systems, Solar Energy 71(2) (2001) 121-133.
[56] J.N. Arnold, I. Catton, D.K. Edwards, Experimental investigation of natural convection in inclined rectangular regions of differing aspect ratios, ASME J. Heat Transfer 98 (1976) 67-71.
[57] CK. Hsieh, Thermal analysis of CPC collectors, Solar Energy 27 (1981) 19-29.
[58] A.F. Kothdiwala, B. Norton, P.C. Eames, The effect of variation of angle of inclination on the performance of low-concentration-ratio compound parabolic concentrating solar collectors, Solar Energy 55(4) (1995) 301-309.
[59] J. Rasoul, P. Prinos, Natural convection in an inclined enclosure, Int. J. Num. Methods Heat Fluid Flow 7(5) (1997) 438-478.

Table 1

Researcher(s)	Details of CPC solar collector	Orientation of collector and parametric range	Assumptions and boundary conditions employed
Tatara and Thodos [49]	Flat plate truncated CPC with concentration ratio (*CR*) of 4 (full height *CR*=5), 2440×31.75×155.5 mm	Horizontal CPC, $1\times10^7 \leq Ra \leq 4\times10^7$	Isothermal absorber and aperture cover (aluminised acrylic film) , both isolated from side and end walls; 0.38 mm thick aluminium side walls
Prapas et al. [10]	CPC with tubular absorber, $CR = 1.56, 2.67, 4.13$	Transversely tilted CPC with $A_x = 1.03, 1.31, 3.16$, $A_z = 4.77, 9.38, 38.17$ and $W = 129.75, 83.88, 49$ mm, $H = 126, 64, 15.5$ mm, ϕ=0,10,20,30^o , $\Delta T = 21.8 - 81.6^\circ C$, $2\times10^3 \leq Gr_d \leq 6\times10^3$	Observed steady state temperature field in cavity air space using Mach-Zehnder interferometer; isothermal absorber; reflector and aperture cover made from continuous duralumin sheet
Fasulo et al. [53]	CPC with a surface area of $0.5\,\mathrm{m}^2$	Horizontal CPC, T_h=100 ˚C	Aluminum deposited glass reflector and glass receiver tube; fluid inlet temperature varied between $60-150^\circ C$ in steps of $15^\circ C$
Eames and Norton [12]	Mach-Zehnder interferometry on CPC with tubular absorber and *CR*=1.154,1.414,2	Transversely tilted CPC *L*=630 mm, *W*=66 mm, *H*=55 mm with $A_x = 1.2$ and $A_z = 11.5$, ϕ=20,30,45^o	Two-dimensional natural convection, uniform temperature along the absorber tube length, one-dimensional conduction in reflector walls, Boussinesq approximation invoked, spatial variation (±10%) of radiation intensity at the aperture cover during experiment
Yadav et al. [54]	CPC with flat plate tube-in-fin type absorber with *CR*=1.7, θ_a=36º	Transversely tilted (ϕ=26.167^o) CPC with *L*=2000 mm, *W*=340 mm, *H*=100 mm, A_x=3.4, A_z=20	Temperature field in air cavity observed using thermocouples; longitudinal axis held horizontal
Eames et al. [55]	CPC with $CR = 2$ ($\theta_a = 30^o$) with inverted tube-in-fin flat plate absorber	Horizontal absorber	Transient two-dimensional natural convection; solar simulator with 7 lamps; validation of numerical results reported only at system boundaries

Table 1. Previous experimental studies detailing natural convection in CPC and V-trough solar collector cavities

Table 2

Researcher(s)	Modelling approach used and details of CPC solar collector	Orientation of collector and parametric range	Assumptions and boundary conditions employed
Rabl [3]	Analytical, CPC with flat plate absorber	Horizontal CPC	Employed correlation based on simple relations involving hot horizontal and vertical plates; heat exchange between the absorber and reflector neglected; isothermal collector components
Abdel-Khalik et al. [7,8]	Finite element method, CPC with flat plate absorber	Transversely tilted (ϕ= 0-60^o) CPCs with A_x=0.18, 0.26, 0.44 for full, 2/3 and 1/3 height CPC with CR=10; A_x=1.91, 1.11, 0.77 for 1/3, 2/3 and full height CPC with CR=2, $1\times10^3 \le Ra \le 2.5\times10^6$	Two-dimensional steady natural convection; isothermal aperture and absorber plate; perfectly reflecting and adiabatic side walls; perfectly transmitting cover; Boussinesq approximation invoked
Hsieh [57]	Analytical, CPC with tubular absorber in an evacuated tube	Horizontal CPC	Two-dimensional steady state thermal analysis; isothermal aperture, reflector and absorber plate; back loss and long and short wave radiation at reflector wall neglected
Prapas et al. [5]	Analytical, CPC with tubular absorber in an evacuated envelope	Horizontal CPC with CR=1.55, 2.75, 4.22 and 5.5 with A_x= 2.44, 1.32, 0.95	CPC assumed as an eccentric horizontal cylinder in an outer cylinder configuration; isothermal absorber, neglected convection between reflector and aperture cover
Chew et al. [45]	CPC with cylindrical absorber (CR=2)	Horizontal CPC with 1000×W×(190,126.6,95,63.3) mm	Isothermal copper absorber and aperture cover, both Nickel chrome plated with emissivity of 0.08-0.09
Chew et al. [11]	Finite element method, CPC with tubular absorber , $CR = 2$	Transversely tilted CPC (ϕ=0,15,30,60,90^o) with $H = 55$ mm, ΔT=20 ˚C for Ra=2.5×10^5	Two dimensional natural convection, adiabatic reflector walls, isothermal aperture cover and absorber, radiative heat transfer within the cavity neglected
Eames and Norton [12]	Primitive variable finite element formulation, tubular absorber type CPC (CR=2, 1.14, 1.154) , absorber diamter 15mm,	Transversely tilted CPC (ϕ=20, 30, 40, 45^o) with L=630 mm, W=66 mm, H=55 mm, A_x=1.2, A_z=11.5, Ra=2.2×10^6	Employed realistic temperature profiles in the absorber and the aperture cover
Eames and Norton [13]	Finite element method, CPC with CR=1.15,1.41 & 2 and tubular absorber	Transversely tilted CPC ϕ=0,15,45^o, $T_h \le 70$ and $\Delta T = 25°C$, $Gr = 3.1\times10^6$	Two-dimensional natural convection; two boundary conditions of adiabatic and realistic heat loss conditions at the reflector walls
Kothdiwala et al. [58]	Analytical, cusp shaped CPC with selectively coated tube-in-envelope type absorber, $CR = 1.5$	Transversely tilted CPC with $L = 1000$ mm ϕ=0-50^o	Studied overall steady thermal performance; 3×10^{-3} mm thick aluminum reflector surface; aperture cover, receiver, envelope and reflector walls assumed at uniform temperatures, back loss assumed as 10% of that from aperture cover to ambient

Table 2. Previous analytical and numerical studies detailing natural convection in CPC and V-trough solar collector cavities

Figure Captions

Fig. 1. Heat exchange processes in CPC solar collectors

Fig. 2. Differently oriented enclosures; (a) horizontally (θ= ϕ= 0°) (b) vertically (θ= 0°, ϕ= 90°) (c) longitudinally (θ> 0°, ϕ= 0°) (d) transversely (θ= 0°, ϕ> 0°)

Fig. 3. Cross-sections of CPC and V-trough solar collectors studied in previous research

Fig. 4. Convective flow patterns in a 60º acceptance half-angle CPC tilted transversely at ϕ = 30º with boundary conditions (a) side walls with realistic backloss (b) adiabatic side walls [13]

Fig. 5. Variation of the Nusselt number with the Rayleigh number for horizontally oriented (θ=ϕ= 0°) rectangular, CPC and V-trough solar collector and cylindrical annuli cavities

Fig. 6. Variation of the Nusselt number with the Rayleigh number for rectangular, CPC and V-trough solar collector cavities transversely tilted at 10º

Fig. 7. Variation of the Nusselt number with the Rayleigh number for 45º transversely tilted rectangular, CPC and V-trough solar collector cavities

Fig. 8. Variation of the Nusselt number with transverse tilt angle at Ra =1×10^5 for $A_x \leq 2$ for rectangular, CPC and V-trough solar collector and cylindrical annuli cavities

Fig 9. Variation of the Nusselt number with transverse tilt angle at Ra =1×10^6 in rectangular, CPC and V-trough cavities with $A_x \leq 2$

Fig. 10. Variation of the Nusselt number with transverse tilt angle at Ra =1×10^7 for $A_x \leq 2$ in rectangular, CPC and V-trough cavities

Figure 1

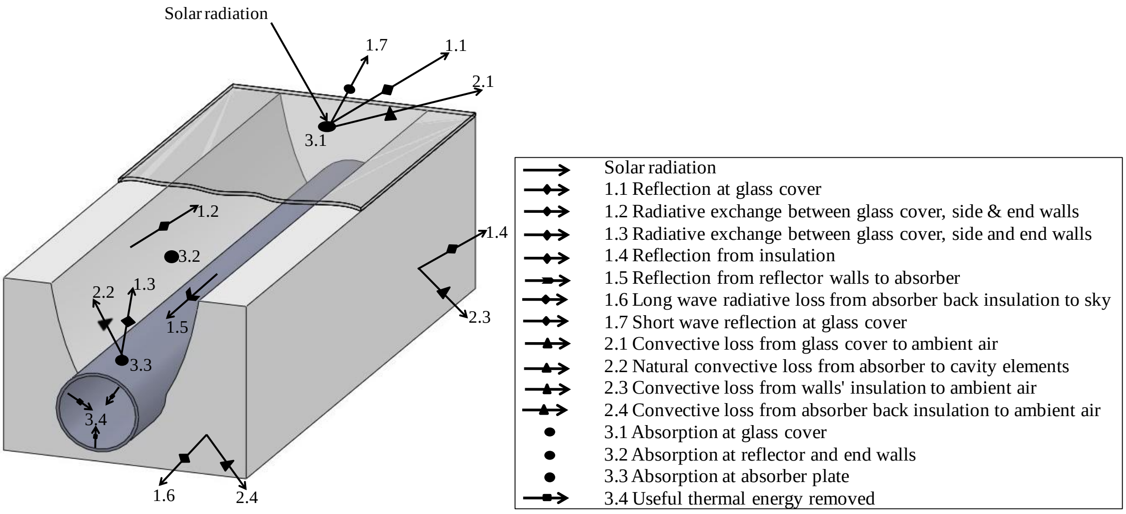

Solar radiation
1.7
1.1
2.1
3.1
1.2
3.2
1.3
2.2
1.5
3.3
3.4
1.4
2.3
1.6
2.4
Solar radiation
1.1 Reflection at glass cover
1.2 Radiative exchange between glass cover, side & end walls
1.3 Radiative exchange between glass cover, side and end walls
1.4 Reflection from insulation
1.5 Reflection from reflector walls to absorber
1.6 Long wave radiative loss from absorber back insulation to sky
1.7 Short wave reflection at glass cover
2.1 Convective loss from glass cover to ambient air
2.2 Natural convective loss from absorber to cavity elements
2.3 Convective loss from walls' insulation to ambient air
2.4 Convective loss from absorber back insulation to ambient air
3.1 Absorption at glass cover
3.2 Absorption at reflector and end walls
3.3 Absorption at absorber plate
3.4 Useful thermal energy removed

Figure 2

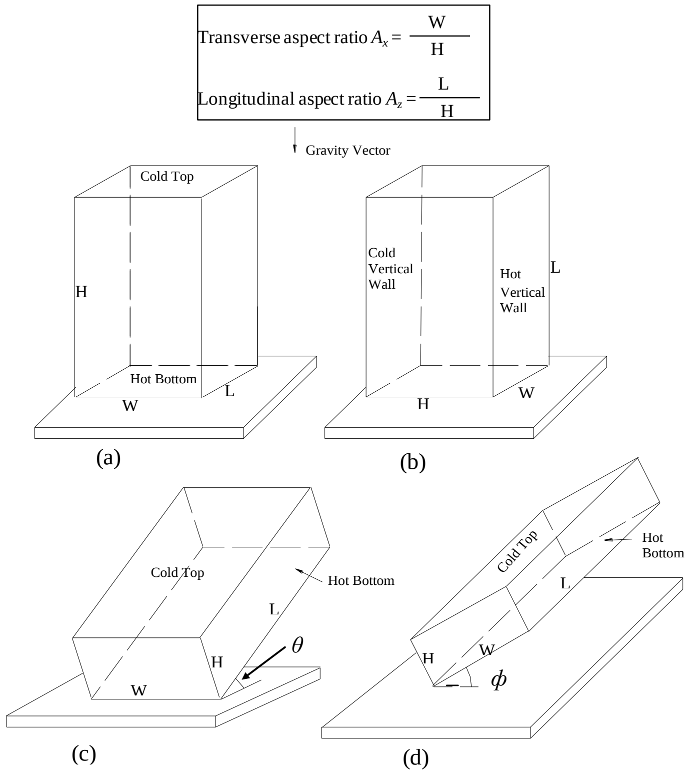

Transverse aspect ratio $A_x = \frac{W}{H}$
Longitudinal aspect ratio $A_z = \frac{L}{H}$
Gravity Vector
Cold Top
H
Hot Bottom
W
L
(a)
Cold Vertical Wall
Hot Vertical Wall
L
H
W
(b)
Cold Top
Hot Bottom
L
θ
H
W
(c)
Cold Top
Hot Bottom
L
H
W
ϕ
(d)

Figure 3

$$\text{Transverse aspect ratio } A_x = \frac{W}{H}$$

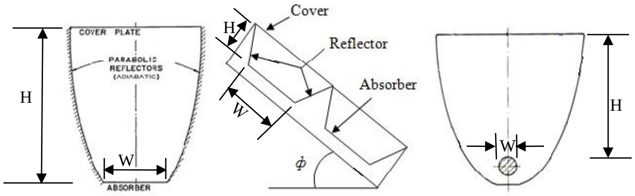

(a) Abdel Khalik et al. [7,8] (b) Meyer et al. [9] (c) Prapas et al. [5,10]

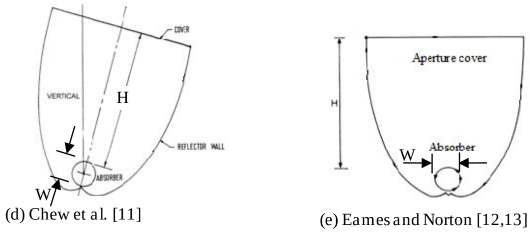

(d) Chew et al. [11]

(e) Eames and Norton [12,13]

Figure 4

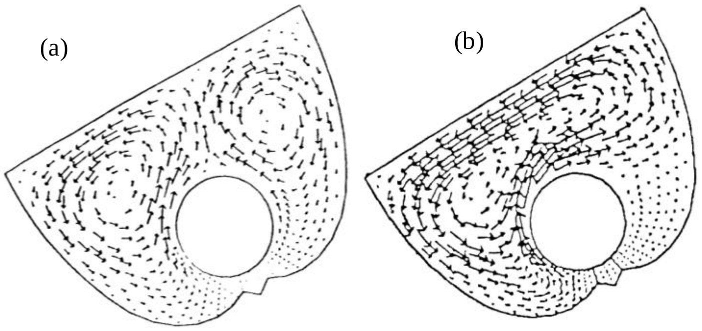

Figure 5

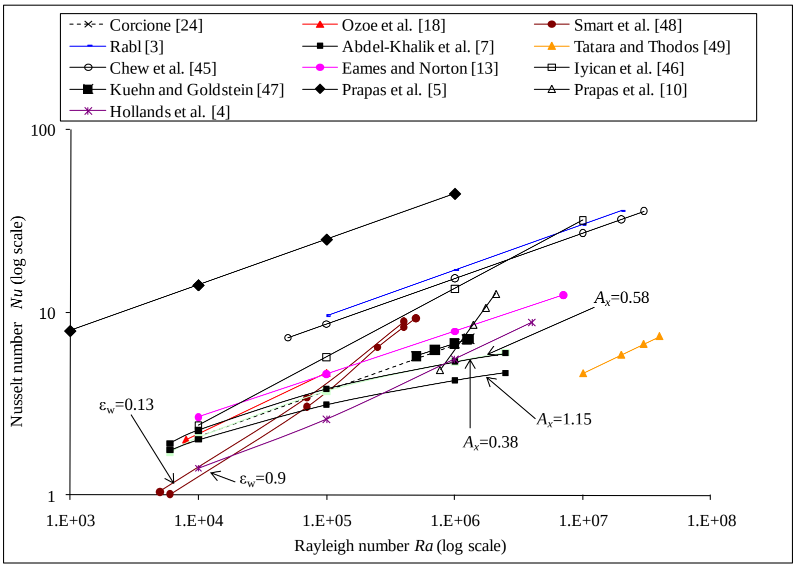

Corcione [24]
Ozoe et al. [18]
Smart et al. [48]
Rabl [3]
Abdel-Khalik et al. [7]
Tatara and Thodos [49]
Chew et al. [45]
Eames and Norton [13]
Iyican et al. [46]
Kuehn and Goldstein [47]
Prapas et al. [5]
Prapas et al. [10]
Hollands et al. [4]
100
10
1
Nusselt number Nu (log scale)
εw=0.13
εw=0.9
Ax=0.58
Ax=1.15
Ax=0.38
1.E+03
1.E+04
1.E+05
1.E+06
1.E+07
1.E+08
Rayleigh number Ra (log scale)

Figure 6

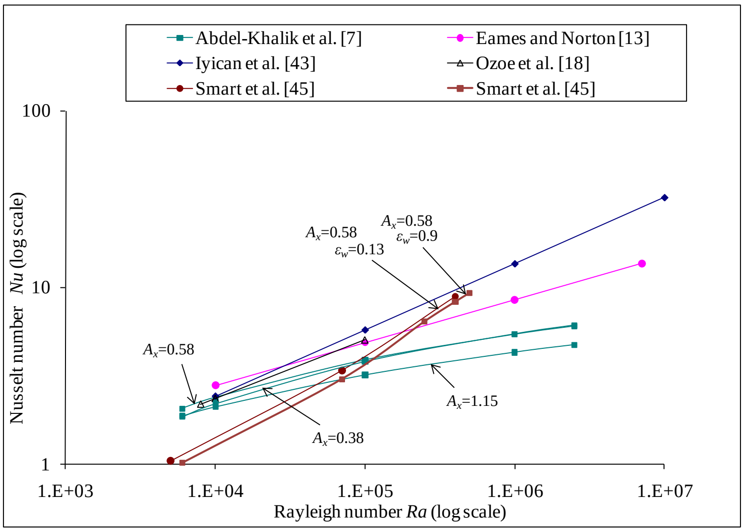
Abdel-Khalik et al. [7]
Eames and Norton [13]
Iyican et al. [43]
Ozoe et al. [18]
Smart et al. [45]
Smart et al. [45]
Nusselt number Nu (log scale)
100
10
1
1.E+03
1.E+04
1.E+05
1.E+06
1.E+07
Rayleigh number Ra (log scale)
Ax=0.58 εw=0.13
Ax=0.58 εw=0.9
Ax=0.58
Ax=0.38
Ax=1.15

Figure 7

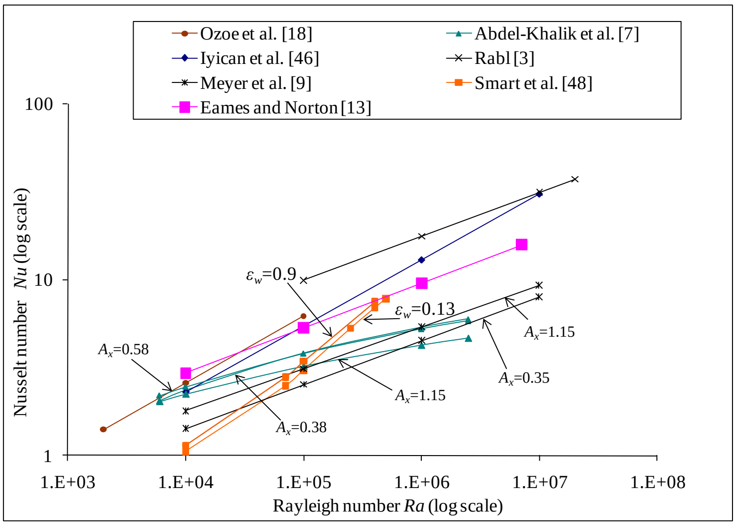

Ozoe et al. [18]
Abdel-Khalik et al. [7]
Iyican et al. [46]
Rabl [3]
Meyer et al. [9]
Smart et al. [48]
Eames and Norton [13]
100
10
1
Nusselt number Nu (log scale)
εw=0.9
εw=0.13
Ax=0.58
Ax=1.15
Ax=0.35
Ax=1.15
Ax=0.38
1.E+03
1.E+04
1.E+05
1.E+06
1.E+07
1.E+08
Rayleigh number Ra (log scale)

Figure 8

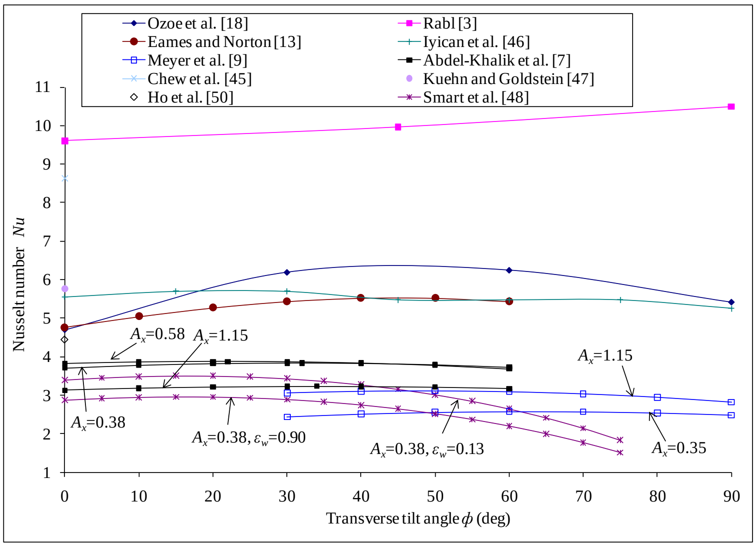

Ozoe et al. [18]
Rabl [3]
Eames and Norton [13]
Iyican et al. [46]
Meyer et al. [9]
Abdel-Khalik et al. [7]
Chew et al. [45]
Kuehn and Goldstein [47]
Ho et al. [50]
Smart et al. [48]
Nusselt number Nu
Transverse tilt angle ϕ (deg)
Ax=0.58
Ax=1.15
Ax=0.38
Ax=0.38, εw=0.90
Ax=0.38, εw=0.13
Ax=1.15
Ax=0.35

Figure 9

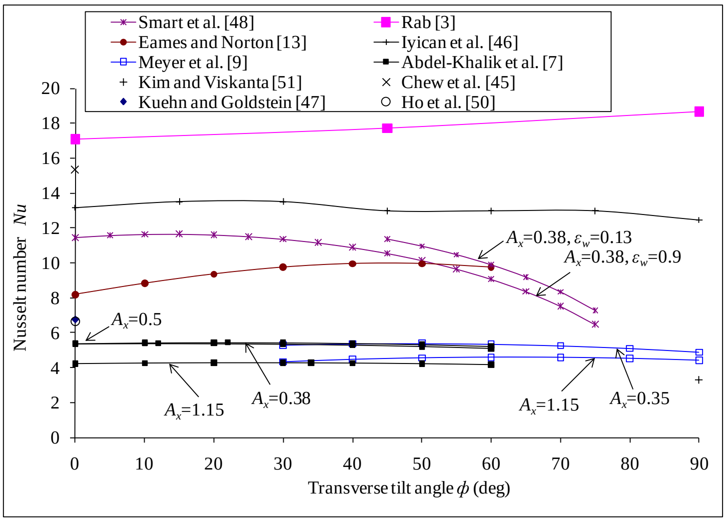
Smart et al. [48]
Rab [3]
Eames and Norton [13]
Iyican et al. [46]
Meyer et al. [9]
Abdel-Khalik et al. [7]
Kim and Viskanta [51]
Chew et al. [45]
Kuehn and Goldstein [47]
Ho et al. [50]
Nusselt number Nu
Transverse tilt angle ϕ (deg)
Ax=0.38, εw=0.13
Ax=0.38, εw=0.9
Ax=0.5
Ax=1.15
Ax=0.38
Ax=1.15
Ax=0.35
0
2
4
6
8
10
12
14
16
18
20
0
10
20
30
40
50
60
70
80
90

Figure 10

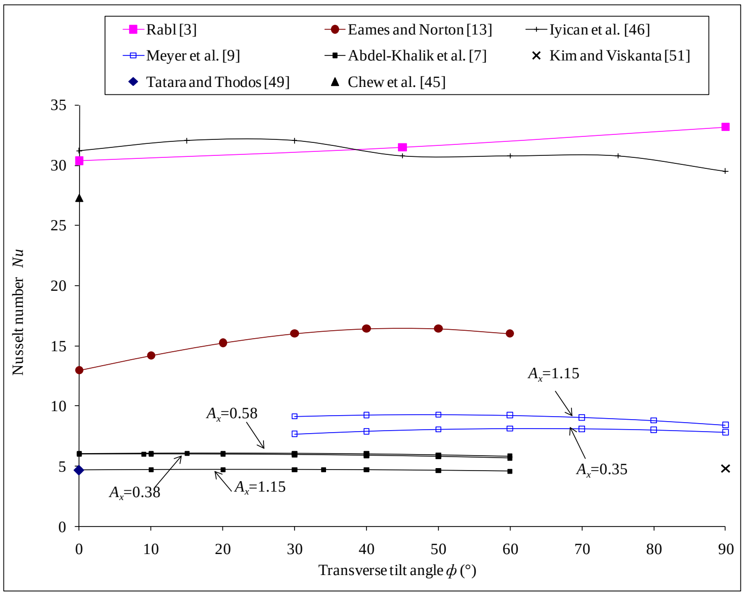

Rabl [3]
Eames and Norton [13]
Iyican et al. [46]
Meyer et al. [9]
Abdel-Khalik et al. [7]
Kim and Viskanta [51]
Tatara and Thodos [49]
Chew et al. [45]
35
30
25
20
15
10
5
0
Nusselt number Nu
A_x=1.15
A_x=0.58
A_x=0.35
A_x=0.38
A_x=1.15
0
10
20
30
40
50
60
70
80
90
Transverse tilt angle ϕ (°)